Science and Technology Indonesia
e-ISSN:2580-4391 *p*-ISSN:2580-4405
Vol. 8, No. 1, January 2023

Research Paper

Photocatalytic Degradation of Rhodamine-B by Ni/Zn LDH Intercalated Polyoxometalate Compound

Yulizah Hanifah[1], Risfidian Mohadi[1,2], Mardiyanto[3], Aldes Lesbani[1,2*]

[1]*Graduate School of Mathematics and Natural Sciences, Faculty of Mathematics and Natural Sciences, Universitas Sriwijaya, OganIlir, 30662, Indonesia*
[2]*Research Center of Inorganic Materials and Coordination Complexes, Faculty of Mathematics and Natural Sciences, Universitas Sriwijaya, OganIlir, 30662, Indonesia*
[3]*Department of Pharmacy, Faculty of Mathematics and Natural Sciences, Universitas Sriwijaya, Ogan Ilir, 30662, Indonesia*
***Corresponding author**: aldeslesbani@pps.unsri.ac.id

Abstract
NiAl-LDH and ZnAl-LDH intercalated polyoxometalate $K_4[SiW_{12}O_{40}]$ and $K_3[PW_{12}O_{40}]$ were synthesized to form composite NiAl-$[SiW_{12}O_{40}]$, NiAl-$[PW_{12}O_{40}]$, ZnAl-$[SiW_{12}O_{40}]$, and ZnAl-$[PW_{12}O_{40}]$. The physicochemical properties of the materials were characterized by XRD, FTIR, SEM, and UV-DRS. The material used for degraded Rhodamine B (RhB) as a cation dye. The results successfully synthesized by showed the peak diffractions angles at 11.63°, 23.13°, and 35.16° for NiAl-LDH and diffractions at 10.39°, 20.17°, 34.6° and 60.52°for ZnAl-LDH. The LDH-typical structure of the composite materials NiAl-$[SiW_{12}O_{40}]$ and NiAl-$[PW_{12}O_{40}]$ was demonstrated by apparent diffraction at 2θ angles of 10.76°, 26.59°, 30.8°, and 63.11° for NiAl-$[PW_{12}O_{40}]$, 2θ angles at 8.26°, 11.34°, 29°, and 35.1° for NiAl-$[SiW_{12}O_{40}]$, 7.73°, 28.6° and 35.6° for ZnAl-$[PW_{12}O_{40}]$, and 8.61°, 25.27°, 34.96° and 66.34° for ZnAl-$[SiW_{12}O_{40}]$. The materials were characterized as an advanced catalyst to improve photocatalytic activity for RhB elimination under visible light sources. The intercalation of polyoxometalate $[SiW_{12}O_{40}]$4- and $[PW_{12}O_{40}]$3- into LDH could enhance the degradation cationic dye of RhB. Intercalation improved the photodegradation performance determined under UV-Vis irradiation conditions which composite NiAl-LDH was better than ZnAl-LDH composite. It was present by the %degradation RhB performances NiAl-LDH, ZnAl-LDH, NiAl-$[SiW_{12}O_{40}]$, NiAl-$[PW_{12}O_{40}]$, ZnAl-$[SiW_{12}O_{40}]$, and ZnAl-$[PW_{12}O_{40}]$ were 91.48%, 88.59%, and 88.41%, and 87.87%, respectively. The %degradation for NiAl-LDH and ZnAl-LDH was 68.94% and 65.76%. Recovery and reusability experiment of the catalyst demonstrated by degradation percentage that the LDH intercalated polyoxometalate has a great photocatalytic ability.

Keywords
LDH, Polyoxometalate, Photocatalytic, Rhodamine-B

Received: 7 Oktober 2022, Accepted: 9 January 2023
https://doi.org/10.26554/sti.2023.8.1.93-99

1. INTRODUCTION

Dyestuffs are organic substances, applied in many industrial sectors such as cosmetics, ink, paint, and textile that cause environmental contamination with toxic compounds (Ahsaine et al., 2018). Rhodamine B (RhB) is one of the cationic dyes that have a group of heterocyclic organic compounds (organic xanthenes dye) and this dye's effluent produces a lot of organic contaminants that are difficult to biochemically degrade and has hazardous carcinogenic for human (Xiang et al., 2018; Wang et al., 2018). Various techniques have been employed to remove such pollutants from wastewater including, electrolysis, oxidation process, adsorption, and photocatalysis. Photodegradation from wastewater is required due to high efficiency and environmental friendliness (Abideen and Teng, 2020).

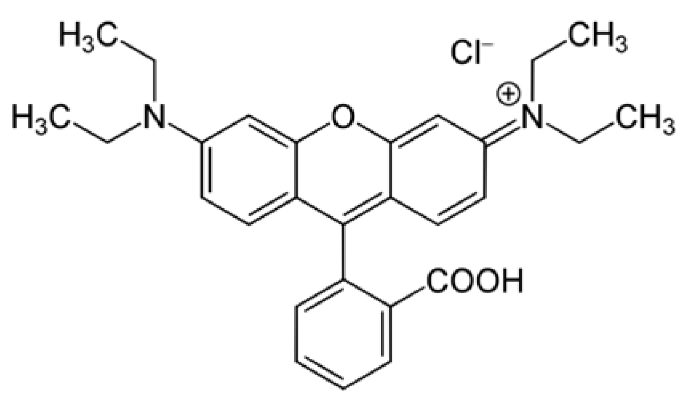

Figure 1. Rhodamine-B's Molecular Structure

Layered double hydroxides (LDHs), consisting of brucite-like layers have also gained substantial interest due to their uses in numerous industries, such as water treatment for the removal of pollutants (Syah et al., 2021). The general formula of LDH M_{1-x}^{2+} M_x^{3+} $(OH)_2]^{x+}$ $(A^n)_{x/n}$.mH_2O where M^{2+} and M^{3+} are divalent metal cations, x is the molar ratio of trivalent cations, A^{n-} is the anion within the interlayer. The structure and characteristics of LDH give wide applications such as adsorbent, ion exchange, and photocatalyst (Das, 2021; Lesbani et al., 2021; Gascho et al., 2019).

The ongoing study in the field of photocatalysts, and their ability as a catalyst in wastewater from pollutants has been degraded using organic materials (Zhang et al., 2014). Consequently, it makes sense to discover efficient methods of treating water pollution. Modification material layered such as LDH for photocatalytic have achieved a certain result due to the excellent properties of LDH in improved ability as a photocatalyst. Polyoxometalate $PW_{12}O_{403}$- intercalated NiFe LDH informed a great ability in water oxidation (Xue et al., 2020). Fe doping on ZnAl-LDH successfully adsorbs and degrades cationic dye (Xu et al., 2018). Another research that used LDH as a photocatalyst was by Xu et al. (2019) the rare earth element combined with LDH could endow the ability as a photocatalyst. MgAlCe-LDHs used a variation ratio of Ce^{2+} successfully degrade methylene blue. Pt modified ZnAl-LDH as a photocatalyst that effectively degrades ciprofloxacin (Li et al., 2020). CoAl-Bi_2O_3 composite successfully degrade rhodamine-B was the highest degradation up to 90.36% (Zhang et al., 2021). MgAl-CrO_{42} efficiently enhanced methylene blue degradation performance (Qing et al., 2021).

Several reports on the invention and use of LDH nanocomposite have been reported in recent years. These nanocomposites were created using various synthetic techniques, including the reconstitution of the coprecipitation synthetic pathway and the ion exchange pathway. Strategies for invention LDH-based materials are used to improve their performance in any application (Miao et al., 2020). The LDH intercalated polyoxometalate composites have several uses in catalytic reactions, like oxidation reactions. According to Amini et al. (2018) inform succeeded in the synthesis of MgAl-POM which was applied to dissolve rhodamine-B and methylene blue, and the degradation rates were 97% and 99%, respectively. Hanifah et al. (2023) successfully modified polyoxometalate with MgAl-LDH for the degradation of the cationic dye malachite green. With 100% conversion and selectivity, the synthetic LDH-PWFe catalyst informed the highest efficiency in the oxidation of benzyl alcohol into benzaldehyde and for LDH-PWZn informed 85% selectivity (Hasannia and Yadollahi, 2015). Wu et al. (2018) successfully synthesized FePW/LDHs and MnPW/LDHs by anion exchange method, the sample exhibited high catalytic activity in degraded MB and AR27 due to the tunable surface charge of the catalyst.

LDH has diverse morphological advantages, adjustable material, to produce a composite, utilizes large interlayer gaps and exchangeable anionic in the interlayer and another functional potential could be used as a photocatalyst (Wu et al., 2018; Zhang et al., 2020; Hanifah et al., 2022) due to the abundance of positive charge also produce more active sites. LDH is a suitable anion exchange material because it allows anions and water molecules to move freely and be changed out readily.

Accordingly, this research aims to develop an efficient photocatalyst composed both of NiAl-LDH and ZnAl-LDH with two different polyoxometalates (POM) type Keggin K_3-[PW_{12} O_{40}] and K_4-[$SiW_{12}O_{40}$] which have different charges by using an ion-exchange approach which resulted in NiAl-[$SiW_{12}O_{40}$], NiAl-[$PW_{12}O_{40}$], ZnAl-[$PW_{12}O_{40}$], and ZnAl-[$SiW_{12}O_{40}$] composite. All the synthesized and ready-made materials were characterized using FTIR, XRD, SEM, and UV-DRS. The high negative charge of polyoxometalate anions for enhancing the capability to degrade RhB. This research evaluated the photodegradation process, including the impact of pH, catalyst loading, contact time, and material regeneration, on the photodegradation of RhB in visible light.

2. EXPERIMENTAL SECTION

2.1 Material and methods

LDH pristine intercalated Keggin-type polyoxometalate was made by the following (Danafar and Yadollahi, 2009). The synthesis used an ion exchange pathway. Materials were characterized using a variety of methods, including the Rigaku XRD Miniflex-6000 diffractometer. Analysis of IR was conducted using Shimadzu FTIR Prestige-21. The degradation of RhB was analyzed by UV-Vis Biobase BK-UV 1800 PC spectrophotometer at 564 nm (Koppala et al., 2021). Band gap energy was provided by UV-DRS using JASCO V-760 and the characterization, morphology material was carried out utilizing SEM Quanta-650 Oxford Instrument. Both polyoxometalate Keggin types of $K_3[PW_{12}O_{40}]$ and $K_4[SiW_{12}O_{40}]$ were created using synthesis according to the procedure (Lesbani and Mohadi, 2014).

2.2 Synthesis of NiAl-LDH

A mixture of 100 mL of aluminum nitrate 0.25 M and 100 mL of nickel nitrate 0.75 M was mixed and stirred for 30 minutes. The mixture's pH was changed by adding 2M of sodium hydroxide. Which was then stirred for 24 hours at 70°C. The material then was filtered, washed, and dried in an oven at 80°C. The substance was examined utilizing an XRD, FT-IR, SEM and UV-DRS.

2.3 Synthesis of ZnAl-LDH

According to Lesbani et al. (2021) improved coprecipitation approach, the synthesis of ZnAl-LDH material was carried out.100 mL aluminum nitrate 0.25 M and 100 mL Zinc Nitrate 0.75 M were combined and stirred for two hours. By adding sodium hydroxide (2M), the mixture's pH was presented to pH 10, then it was stirred for 18 hours at 85°C. Then, the precipitation was filtered, washed, and dried in an oven set up to 80°C.

2.4 Preparation of Composite

Intercalated materials were prepared by using the ion exchange method. Polyoxometalate intercalated LDH layer was carried out by creating solution A by mixing 25 mL of distilled water with 1 g of polyoxometalate and solution B of 2 g of LDH added with 25 mL sodium hydroxide 1 M. Solution A and B were mixed rapidly under conditions of N_2 gas for 2 days. The precipitate was filtered, washed, and dried using an oven at a temperature of 80°C for 12 hours. The prepared materials were characterized using XRD, FT-IR, SEM, and UV-DRS.

2.5 Photocatalytic Activity

The material was applied as a photocatalyst. Typically, adding 2 mg of the photocatalyst is into 20 mL of dye solution (RhB 10 mg/L) and stirred in the dark for 1 hour to reach an adsorption-desorption equilibrium. The mixture was irradiated by visible light for 2 hours. The examined optimum of degradation in this study was applicated variation pH at 1, 3, 5, 7, and 9; catalyst weight at 0.075, 0.1, 0.25, 0.5, and 0.75 g and contact time at 10, 20, 30, 40, 50, 60, 70, 80, 90, 100, 110, and 120 minutes. RhB dye concentration was measured in the solution using UV-Vis spectrophotometry by measuring the absorbance at 564 nm (Koppala et al., 2021). The use of the treated solution yielded photocatalyst then washed, and dried at 100°C. The photocatalyst was repeated under the same condition to examine the regeneration. Using the expression, the effectiveness of dye degradation was estimated.

$$\%\text{Degradation} = \frac{(\text{Co} - \text{Ct})}{\text{Co}} \times 100\% \quad (1)$$

where Co is the initial dye concentration and Ct is the adsorb at time t.

3. RESULT AND DISCUSSION

3.1 LDH Pristine and LDH Composite Characterization

NiAl LDH and ZnAl LDH as LDH pristine and were synthesized and characterized. Figure 2 shows the XRD pattern for LDH pristine and LDH composite before the degradation process. The XRD pattern of the LDH composite also showed in Figure 2. The XRD diffractions of the material confirmed the good formation characteristic of the LDH structure. Then all materials are compared in Figure 2. The peak observed at 11.63°, 23.13°, and 35.16° for NiAl-LDH and 10.39°, 20.17°, 34.6° and 60.52°for ZnAl-LDH, material pristine was successfully synthesized. The study of Wang et al. (2018) for the original diffraction of $K_3[\alpha\text{-}PW_{12}O_{40}]$ was shown at range 2θ angles of 5-10°, 10-20°, and 25-30°. The composite material was successfully intercalated by showing peak polyoxometalate material on NiAl-$[PW_{12}O_{40}]$, it was showing a peak at angles 10.76°, 26.59°, 30.8° and 63.11°. The similar case in composite material of NiAl-$[SiW_{12}O_{40}]$ that indicated at peak 8.26°, 11.34°, 29°, and 35.1°. The diffraction peak at 7.73°, 28.64° and 35.63° for ZnAl-$[PW_{12}O_{40}]$. The presence of -$[SiW_{12}O_{40}]$ in LDH composite is indicated at 2θ angles 8.61°, 24.27°, 34.96° and 66.34°for ZnAl-$[SiW_{12}O_{40}]$. Hanifah et al. (2022) indicated from Siregar et al. (2022) the characteristic LDH structure shown (003), (006), (009) at 2θ angle 11.47°, 22.6°and 34.69° and indicated the anion on the interlayer structure on (110) at an angle 61.62°. A typical principal diffraction peak shown on each material either LDH pristine ensure that the crystal plane (003), (006), (012), (015), (018), (110), and (113) correspond to complete the synthesis (Normah et al., 2021).

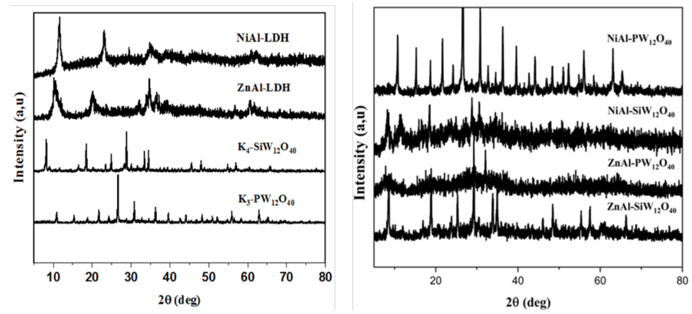

Figure 2. Catalyst Diffractogram of NiAl-LDH, ZnAl-LDH, K3 $[PW_{12}O_{40}]$, $K_4[SiW_{12}O_{40}]$, NiAl-$K_3[PW_{12}O_{40}]$, NiAl-$K_4[SiW_{12}O_{40}]$, ZnAl-$K_4[SiW_{12}O_{40}]$, and ZnAl-$K_4[PW_{12}O_{40}]$

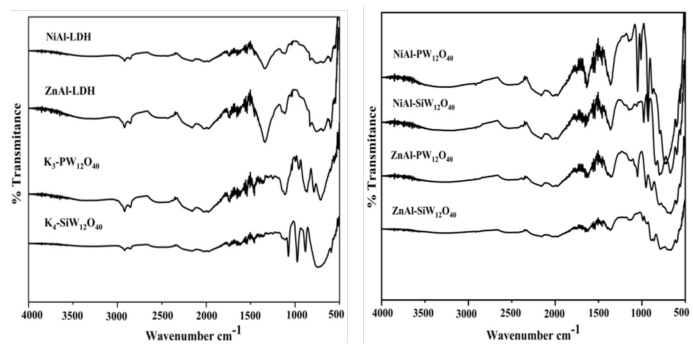

Figure 3. FTIR Spectra of Catalyst

The FTIR spectra of the functionalized composites and all LDH pristine were present in Figure 3 within a recording range of 4000 to 400 cm^{-1}. The FTIR of LDH pristine NiAl LDH and ZnAl LDH as based material displayed peaks in the range of 3420-3480 cm^{-1} and 1620 to 1640 cm^{-1} corresponding to the stretching vibration of an interlayer water molecule and hydroxyl group vibration. The intercalated NO_3^- bending and the CO_3-vibration mode vibration are present in all of the LDH at 1348 cm^{-1} and 1361 cm^{-1} (Nayak and Parida, 2016). The bending and stretching vibrations M-O and M-O-M and O-M-O are represented by the absorption band in the 500-800 cm^{-1} range in this study show the band 983-870cm^{-1} band 983-870cm^{-1} and 804.84 cm^{-1} respectively (Wang et al., 2018).

Typical SEM image of NiAl-LDH, NiAl-$[SiW_{12}O_{40}]$, NiAl-$[PW_{12}O_{40}]$, ZnAl LDH, ZnAl-$[SiW_{12}O_{40}]$, and ZnAl-$[PW_{12}$

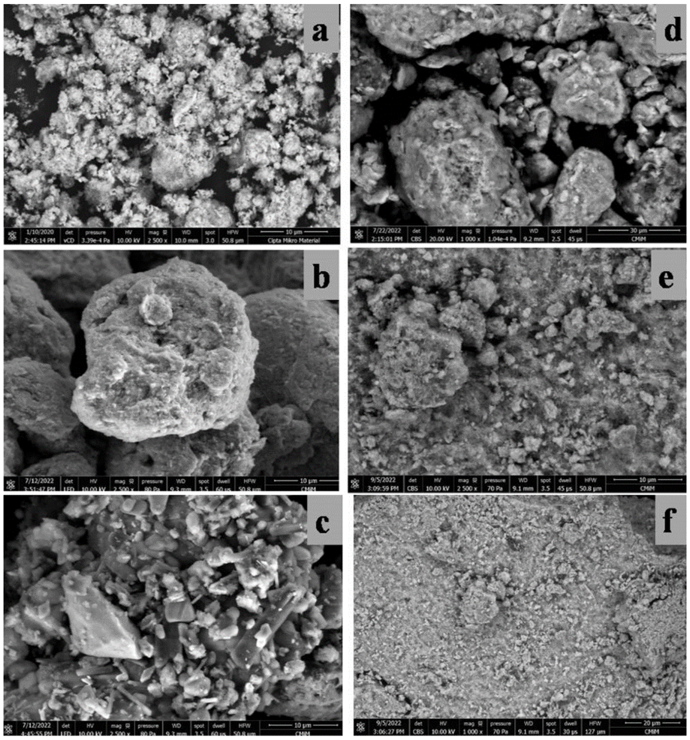

Figure 4. SEM of (a) NiAl-LDH (b) NiAl-$[SiW_{12}O_{40}].nH_2O$ (c) NiAl-$[PW_{12}O_{40}].nH_2O$ (d) ZnAl-LDH (e) ZnAl-$[SiW_{12}O_{40}].nH_2O$ (f) ZnAl-$[PW_{12}O_{40}].nH_2O$

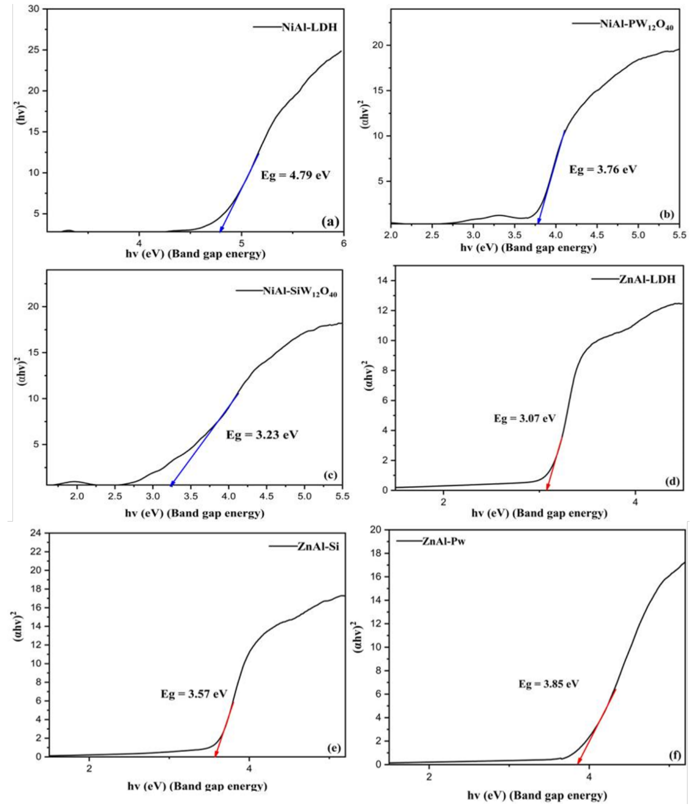

Figure 5. Spectra and Energy Band Gap for UV-DRS of NiAl-LDH (a) NiAl-$[PW_{12}O_{40}]$ (b) NiAl-$[SiW_{12}O_{40}]$ (c) ZnAl-LDH (d) ZnAl-$[PW_{12}O_{40}]$ (e) and ZnAl-$[SiW_{12}O_{40}]$ (f)

$O_{40}]$ powders are depicted in Figure 4. To understand the relationship of the microstructure of the layer composite of LDH. The particle shape is typically spherical and relatively identical to one another. The SEM image shows the powder's size distribution was not identified. Figure 4a shows the random spherical size on the surface. Introducing anionic polyoxometalate decreased the particle size and gained neatly arranged spherical.

Figure 5 shows the UV-DRS pristine and composite's LDH spectrum energies. According to Wijaya et al. (2021), the abscissa value of the NiAl-LDH is *hv* or energy band gap, curve coordinates are valued $(\alpha hv)^2$, where α is the absorptivity coefficient, h is the plank constant and v is the light frequency (Yuliasari et al., 2022). This study used polyoxometalate to composite NiAl-LDH with ZnAl-LDH. The band gap energies of NiAl-$[PW_{12}O_{40}]$, NiAl-$[SiW_{12}O_{40}]$, ZnAl-$[PW_{12}O_{40}]$, and ZnAl-$[SiW_{12}O_{40}]$ were 3.76 eV and 3.23 eV, 3.57 eV, and 3.85 eV respectively. The energy band gap for NiAl-LDH and ZnAl-LDH were 4.79 eV and 3.07 eV. Both band gap energy of NiAl composites is lower than LDH pristine which is NiAl-LDH. Each material corresponds to obtain a greater kap value and %degradation when compared to pure LDH, which has a band gap of The band gap 68.94% degradation, LDH composite exhibits more effective photocatalytic efficiency than NiAl-LDH to 91.48% for NiAl-$[SiW_{12}O_{40}]$ and 88.59% for NiAl-$[PW_{12}O_{40}]$. The results indicated that materials NiAl composite as photocatalysts displayed the appropriate band gap energy (Eg) for the degradation of organic pollutants such as rhodamine-b dye.

3.2 The Effect of pH Variables in Optimization on the Degradation of Rhodamine-b

Additionally, LDH pristine and LDH composite were adjusted for the impact of pH change on LDH degradation by varying pH = 1, 3, 5, 7, and 9 by using 0.1 M of NaOH and 0.1 M HCl. The effect of pH on LDH pristine and LDH composite degradation stability was shown in Figure 6. As the pH decreased, the degradation capacity was increased it came on both material polyoxometalate on degradation rhodamine-b which were $K_4[SiW_{12}O_{40}]$ at pH 1 and $K_3[SiW_{12}O_{40}]$ at pH 1. The anionic depends on the pH medium and total concentration of dye (Kangralkar et al., 2019). The highest ability on NiAl LDH and ZnAl LDH was found at pH 7. The pH optimum composite materials were NiAl-$[SiW_{12}O_{40}]$, NiAl-$[PW_{12}O_{40}]$, ZnAl-$[SiW_{12}O_{40}]$ and ZnAl-$[PW_{12}O_{40}]$ at pH 7, 1, 9, 1. In acidic conditions, there is a strong attraction between the interaction of negatively charged that in this study polyoxometalate ions and the positively charged catalyst of LDH (Kangralkar et al., 2019). The highest capability on acidic pH

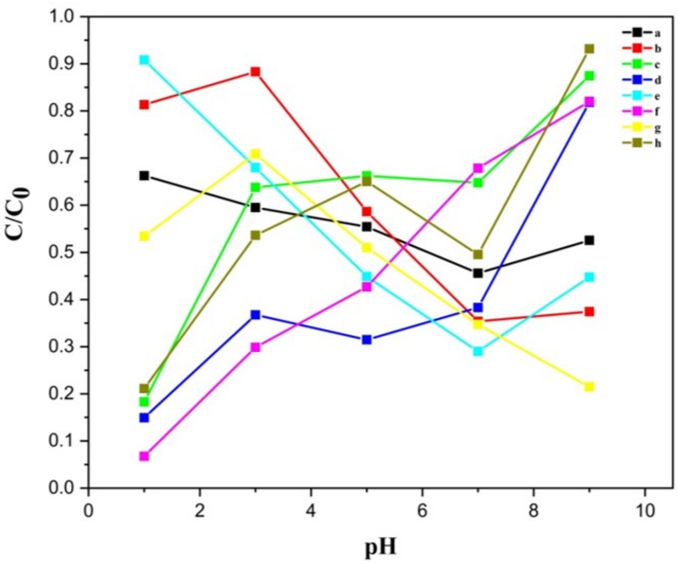

Figure 6. pH's Impact on Catalyst Ability to Degrade RhB by Catalysts a) NiAl-LDH b) ZnAl-LDH c) $K_4SiW_{12}O_{40}$ d) $K_3PW_{12}O_{40}$ e) NiAl-$SiW_{12}O_{40}$ f) NiAl-$PW_{12}O_{40}$ g) ZnAl-$SiW_{12}O_{40}$ and h) ZnAl-$PW_{12}O_{40}$

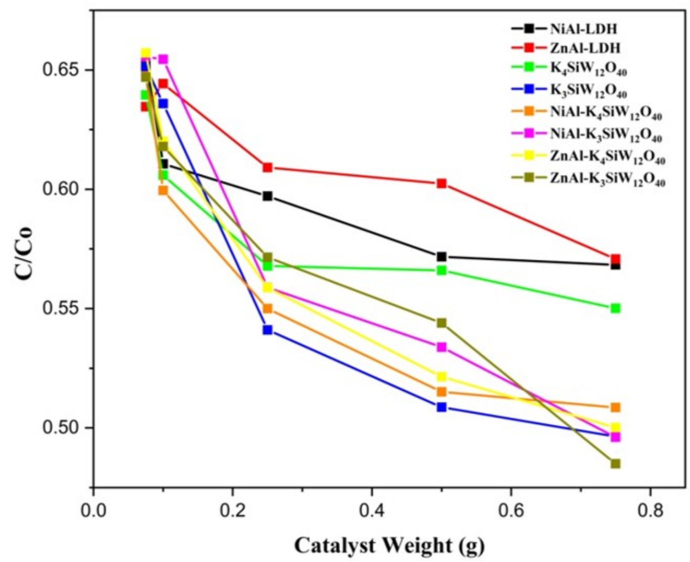

Figure 7. Catalyst Weight Effects on RhB Catalyst Degradation

media might cause generating OH• radicals that are capable of degrading dyestuffs (Elhalil et al., 2018).

3.3 Optimation Catalyst Weight on Degradation

The effect of enhanced catalyst weight performance takes place to prevent a catalyst shortage and excessive catalyst weight. It was examined for all materials used for degradation RhB either anionic polyoxometalate or LDH pristine and LDH composite. For examination, the catalyst weight is used at 0.25 g. Firstly, the material took placed in dark conditions for 30 minutes to calculate %degradation and kinetic parameters. Figure 7 shows the optimum catalyst weight at the ideal pH degradation 120 minutes of conditions for each catalyst of photodegradation. Refraction of light and less light penetration into the solution may result in a minor reduction in catalyst weight above the optimal weight (Elhalil et al., 2018).

3.4 Contact Time's Impact on Photodegradation

The percentage of degradation capacity of rhodamine-b on LDH composite and LDH pristine are shown in Figure 8. The optimum pH and catalyst weight was obtained at pH 7 and 0.75 g for both NiAl LDH and ZnAl LDH. The degradation ability increased by almost up to 2 hours. It showed that the effectiveness of the catalyst in the rhodamine-b degrading procedure had a beneficial outcome. Before turning on UV radiation condition for 120 minutes. The material was done in the reduction condition which was an adsorption process due to it occurring in low light, a procedure of rhodamine-b 10 ppm for 30 minutes to calculate %degradation and kinetic parameters. Figure 8 demonstrates the impact of differences in the amount of time that LDH composite and LDH pristine as basis material take to degrade RhB. There was no significant change in rhodamine-b concentration in an increase in time. In this study, the C/Co value for 20 minutes of treatment had grown with increasing treatment time, which increased the amount of rhodamine-b degraded. The percent rhodamine-b degradation for NiAl-[$SiW_{12}O_{40}$], NiAl-[$PW_{12}O_{40}$], ZnAl-[$SiW_{12}O_{40}$], and ZnAl-[$PW_{12}O_{40}$] was 91.48%, 88.59%, and 88.41%, and 87.87%, respectively. The %degradation for NiAl LDH and ZnAl LDH was 68.94% and 65.76%, respectively. According to the percentage degradation data, the composite catalyst NiAl-[$PW_{12}O_{40}$] and NiAl-[$SiW_{12}O_{40}$] appear to be more effective at RhB degradation than LDH pristine. The degradation percentage carried by theNiAl-[$SiW_{12}O_{40}$] composites was comparable to that of the NiAl-[$PW_{12}O_{40}$] composites.

3.5 Regeneration of Catalyst

The sample's structural stability is one of the key variables affecting real-scale applicability. The cycling ability was determined for this study was fifth times. Even after a fifth run, the sample maintained great efficiency, and it may be used repeatedly to break down organic contaminants. The excellent cycling performance of LDH composite and LDH pristine was detected. Figure 9 shows the different degradation abilities after fifth times repeated use. It is seen that the %degradation was decreased after several cycles used. The last performance ability to degrade RhB of %degradation NiAl-LDH, ZnAl-LDH, NiAl-[$PW_{12}O_{40}$], NiAl-[$SiW_{12}O_{40}$], ZnAl-[$PW_{12}O_{40}$] and ZnAl-[$SiW_{12}O_{40}$] resulted in 58.75, 41.77, 70.65, 67.44, 62.5 and 56.75%, respectively.

4. CONCLUSION

NiAl-LDH and ZnAl-LDH were synthesized using the coprecipitation technique. Based on the characterization results, the

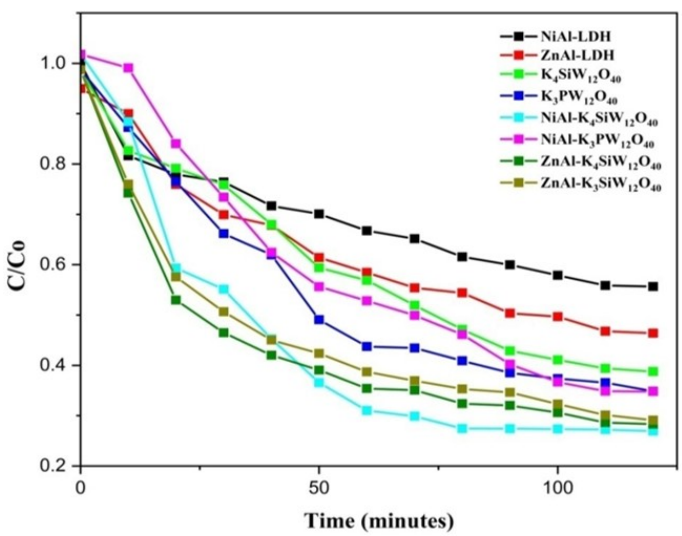

Figure 8. Contact Times Impact on Catalyst's Ability to Degrade RhB

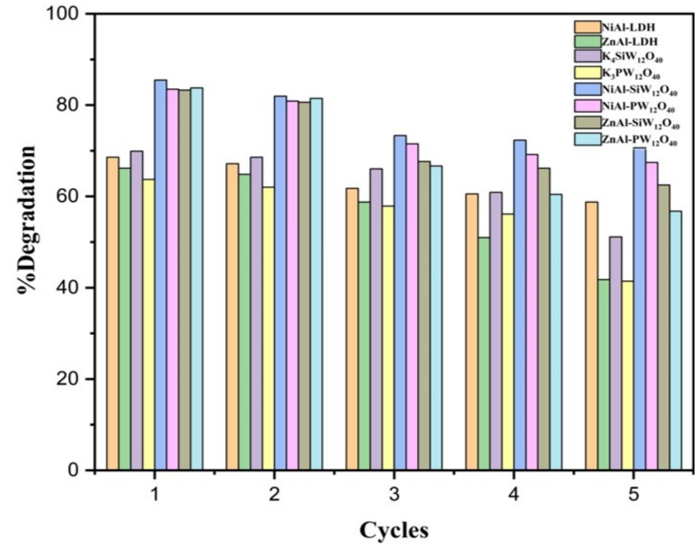

Figure 9. Catalyst Regeneration in the Fifth Cycle

material synthesis conditions for a well-oriented layer structure. The polyoxometalate was intercalated successfully into LDH, and confirmed by analytical technique. Reflected the band gap on the NiAl-LDH composite was better than the ZnAl-LDH composite. The composite is effective as a photodegradation activity on the degradation of rhodamine-b. 10 mg/L of dyes was completely removed after 120 minutes using 0.1 g of catalyst. The synthetic LDH composite and LDH pristine showed enhancement in the photocatalytic removal rhodamine-b by 68.94% for NiAl LDH to 91.48% NiAl-[$SiW_{12}O_{40}$], and 65.76% for ZnAl LDH to 88.41% for ZnAl-[$SiW_{12}O_{40}$], respectively.

5. ACKNOWLEDGMENT

This research was supported by the Ministry of Education, Culture, Research and Technology Republic Indonesia Through Dikti on Hibah Disertasi Doktor with the main contract no. 142/E5/PG.02.00.PT/2022 and derivative contract no. 0145. 005/UN.9.3.1/PL/2022. The authors also thank the Research Center of Inorganic Materials and Complexes FMIPA Universitas Sriwijaya for valuable discussion, apparatus, and chemical analysis.

REFERENCES

Abideen, Z. U. and F. Teng (2020). Fe2O3-Promoted Interface Charge Separation and Visible-light Activity of Fe2O3@ Zn0. 3Cd0. 7S. *Materials Chemistry and Physics*, **246**(2); 122811

Ahsaine, H. A., M. Zbair, Z. Anfar, Y. Naciri, N. El Alem, and M. Ezahri (2018). Cationic Dyes Adsorption Onto High Surface Area 'almond Shell'Activated Carbon: Kinetics, Equilibrium Isotherms and Surface Statistical Modeling. *Materials Today Chemistry*, **8**(3); 121–132

Amini, M., M. Khaksar, A. Ellern, and L. K. Woo (2018). A New Nanocluster Polyoxomolybdate [Mo36O110 (NO) 4 (H2O) 14]· 52H2O: Synthesis, Characterization and Application in Oxidative Degradation of Common Organic Dyes. *Chinese Journal of Chemical Engineering*, **26**(2); 337–342

Danafar, H. and B. Yadollahi (2009). (TBA) 4PFeW11O39· 3H2O Catalyzed Efficient and Facile Ring Opening Reaction of Epoxides with Aromatic Amines. *Catalysis Communications*, **10**(6); 842–847

Das, S. (2021). Superior Photocatalytic Performance of Co Al LDH in the Race of Metal Incorporated LDH: a Comparison Study. *Materials Today*, **35**(4); 275–280

Elhalil, A., M. Sadiq, M. Abdennouri, Y. Kadmi, L. Favier, and N. Barka (2018). Synthesis of Ba doped ZnO/Al2O3 Nanocomposite from Layered Double Hydroxide Structure and Their Photocatalytic Activity for the Degradation of Caffeine. *Journal of Applied Surfaces and Interfaces*, **4**(1-3); 9–16

Gascho, J. L., S. F. Costa, A. A. Recco, and S. H. Pezzin (2019). Graphene Oxide Films Obtained by Vacuum Filtration: X-ray Diffraction Evidence of Crystalline Reorganization. *Journal of Nanomaterials*, **2019**(4); 1–12

Hanifah, Y., R. Mohadi, M. Mardiyanto, and A. Lesbani (2022). Photocatalytic Degradation of Malachite Green by NiAl-LDH Intercalated Polyoxometalate Compound. *Bulletin of Chemical Reaction Engineering & Catalysis*, **17**(3); 627–637

Hanifah, Y., R. Mohadi, M. Mardiyanto, and A. Lesbani (2023). Polyoxometalate Intercalated MgAl-Layered Double Hydroxide for Degradation of Malachite Green. *Ecological Engineering & Environmental Technology*, **24**(2); 109–119

Hasannia, S. and B. Yadollahi (2015). Zn-Al LDH Nanostructures Pillared by Fe Substituted Keggin Type Polyoxometalate: Synthesis, Characterization and Catalytic Effect in Green Oxidation of Alcohols. *Polyhedron*, **99**; 260–265

Kangralkar, M., V. Kangralkar, N. Momin, and J. Manjanna (2019). Cu2O Nanoparticles for Removal of Methylene Blue Dye from Solution. *Environmental Nanotechnology, Monitoring and amp; Management*; 100265

Koppala, S. R., K. Balan, L. Banerjee, H. Li, K. Liu, K. Kumar, V. Raghava, Reddy, and V. Sadhu (2021). Room Temperature Synthesis of Novel Worn Like Tin Oxide Nanoparticle for Photocatalytic Degradation of Organic Pollutants. *Material Science Energy Technologies*, **4**; 113–118

Lesbani, A. and R. Mohadi (2014). Brönsted Acid of Keggin Type Polyoxometalate Catalyzed Pinacol Rearrangement. *Bulletin Chemical Reaction Engineering and Catalysis*, **9**(2); 236–141

Lesbani, A., P. M. S. B. N. Siregar, N. R. Palapa, T. Taher, and F. Riyanti (2021). Adsorptive Removal Methylene-Blue Using Zn/Al LDH Modified Rice Husk Biochar. *Polish Journal of Environmental Studies*, **30**(4); 3117–3124

Li, Z., M. Chen, H. Hu, Q. Zhang, and D. Tao (2020). Mechanochemical Synthesis of Novel Pt Modified ZnAl-LDH for Effective Ciprofloxacin Photodegradation. *Journal of Solid State Chemistry*, **290**(8); 121594

Miao, Y. F., R. T. Guo, J. W. Gu, Y. Z. Liu, G. L. Wu, C. P. Duan, X. D. Zhang, and W. G. Pan (2020). Fabrication of β-In2S3/NiAl-LDH Heterojunction Photocatalyst with Enhanced Separation of Charge Carriers for Efficient CO2 Photocatalytic Reduction. *Applied Surface Science*, **527**(8); 146792

Nayak, S. and K. Parida (2016). Nanostructured CeO2/MgAl-LDH Composite for Visible Light Induced Water Reduction Reaction. *International Journal of Hydrogen Energy*, **41**(46); 21166–21180

Normah, N., N. R. Palapa, T. Taher, R. Mohadi, H. P. Utami, and A. Lesbani (2021). The Ability of Composite Ni/Al-Carbon Based Material Toward Readsorption of Iron (II) in Aqueous Solution. *Science and Technology Indonesia*, **6**(3); 156–165

Qing, X., L. Yuan, Y. Wang, Z. Zhang, M. Bi, and X. Weng (2021). Synergistic Influence of Cr3+ and CrO42- on the Visible Near Infrared Spectrum of Mg-Al Layered Double Hydroxides for Efficient Visible Light Photocatalysis. *Journal of Alloys and Compounds*, **872**; 159628

Siregar, P. M. S. B. N., A. Lesbani, and R. Mohadi (2022). Mg/Al Chitosan as a Selective Adsorbent in The Removal of Methylene Blue from Aqueous Solutions. *Science and Technology Indonesia*, **7**(2); 170–178

Syah, R., A. Al-Khowarizmi, M. Elveny, and A. Khan (2021). Machine Learning Based Simulation of Water Treatment Using LDH/MOF Nanocomposites. *Environmental Technology & Innovation*, **23**; 101805

Wang, Y., F. Song, J. Zhu, Y. Zhang, L. Du, and C. Kan (2018). Highly Selective Fluorescent Probe Based on a Rhodamine B and Furan-2-carbonyl Chloride Conjugate for Detection of Fe3+ in Cells. *Tetrahedron letters*, **59**(42); 3756–3762

Wijaya, A., P. M. S. B. N. Siregar, A. Priambodo, N. R. Palapa, T. Taher, and A. Lesbani (2021). Innovative Modified of Cu-Al/C (C= Biochar, Graphite) Composites for Removal of Procion Red from Aqueous Solution. *Science and Technology Indonesia*, **6**(4); 228–234

Wu, X., C. Ci, Y. Du, X. Liu, X. Li, and X. Xie (2018). Facile Synthesis of NiAl-LDHs with Tunable Establishment of Acid-base Activity Sites. *Materials Chemistry and Physics*, **211**; 72–78

Xiang, L., X. Zhu, L. Kong, H. Zhou, M. Wu, H. Qian, and W. Wang (2018). Small Lanthanide-doped Sr2YbF7 Nanocrystals: Upconversion Fluorescence and Upconversion-driven Photodegradation. *Optical Materials*, **86**; 537–544

Xu, M., B. Bi, B. Xu, Z. Sun, and L. Xu (2018). Polyoxometalate Intercalated ZnAlFe Layered Double Hydroxides for Adsorbing Removal and Photocatalytic Degradation of Cationic Dye. *Applied Clay Science*, **157**; 86–91

Xu, M., G. Pan, Y. Meng, Y. Guo, T. Wu, and H. Chen (2019). Effect of Ce3+ on the Photocatalytic Activity of MAlCe Ternary Hydrotalcites Like Compounds in Methylene Blue Photodegradation. *Applied Clay Science*, **170**; 46–56

Xue, X., F. Yu, J. G. Li, G. Bai, H. Yuan, J. Hou, B. Peng, L. Chen, M. F. Yuen, and G. Wang (2020). Polyoxometalate Intercalated NiFe Layered Double Hydroxides for Advanced Water Oxidation. *International Journal of Hydrogen Energy*, **45**(3); 1802–1809

Yuliasari, N., A. Wijaya, R. Mohadi, E. Elfita, and A. Lesbani (2022). Photocatalytic Degradation of Malachite Green by Layered Double Hydroxide Based Composites. *Bulletin of Chemical Reaction Engineering & Catalysis*, **17**(2); 240–249

Zhang, F., B. Lu, and P. Sun (2020). Highly Stable Ni-based Catalysts Derived from LDHs Supported on Zeolite for CO2 Methanation. *International Journal of Hydrogen Energy*, **45**(32); 16183–16192

Zhang, L., Y. Meng, H. Shen, J. Li, C. Yang, B. Xie, and S. Xia (2021). Photocatalytic Degradation of Rhodamine B by Bi2O3@ LDHs Scheme Heterojunction: Performance, Kinetics and Mechanism. *Applied Surface Science*, **567**; 150760

Zhang, S., Y. Han, L. Wang, Y. Chen, and P. Zhang (2014). Treatment of Hypersaline Industrial Wastewater from Salicylaldehyde Production by Heterogeneous Catalytic Wet Peroxide Oxidation on Commercial Activated Carbon. *Chemical Engineering Journal*, **252**; 141–149

